CHEMISTRY
A EUROPEAN JOURNAL

FULL PAPER

DOI: 10.1002/chem.201300817

Specific Detection and Imaging of Enzyme Activity by Signal-Amplifiable Self-Assembling ^{19}F MRI Probes

Kazuya Matsuo,[a] Rui Kamada,[a] Keigo Mizusawa,[a] Hirohiko Imai,[b] Yuki Takayama,[b] Michiko Narazaki,[b] Tetsuya Matsuda,[b] Yousuke Takaoka,[a] and Itaru Hamachi*[a, c]

Abstract: Specific turn-on detection of enzyme activities is of fundamental importance in drug discovery research, as well as medical diagnostics. Although magnetic resonance imaging (MRI) is one of the most powerful techniques for noninvasive visualization of enzyme activity, both in vivo and ex vivo, promising strategies for imaging specific enzymes with high contrast have been very limited to date. We report herein a novel signal-amplifiable self-assembling ^{19}F NMR/MRI probe for turn-on detection and imaging of specific enzymatic activity. In NMR spectroscopy, these designed probes are "silent" when aggregated, but exhibit a disassembly driven turn-on signal change upon cleavage of the substrate part by the catalytic enzyme. Using these ^{19}F probes, nanomolar levels of two different target enzymes, nitroreductase (NTR) and matrix metalloproteinase (MMP), could be detected and visualized by ^{19}F NMR spectroscopy and MRI. Furthermore, we have succeeded in imaging the activity of endogenously secreted MMP in cultured media of tumor cells by ^{19}F MRI, depending on the cell lines and the cellular conditions. These results clearly demonstrate that our turn-on ^{19}F probes may serve as a screening platform for the activity of MMPs.

Keywords: enzyme activity · imaging agents · magnetic resonance imaging · NMR spectroscopy · self-assembly · signal amplification

Introduction

There are many uses for the specific detection and imaging of enzyme activity in vivo in both drug discovery research and medical diagnostics. Chemical "switchable" probes, which induce detectable signal changes in response to specific enzyme reactions, are particularly useful for imaging enzyme activities because they allow selective and sensitive detection with high signal-to-noise ratios.[1,2] Many fluorescent switching probes for detecting enzyme activities have now been developed.[3] However, fluorescence techniques are, in general, not suitable for in vivo imaging due to the limited light transmission and its scattering in animal bodies. Although magnetic resonance imaging (MRI) is known to be an adequate technique for in vivo studies,[4] switching strategies for MRI are as yet quite limited. As a pioneering example, ^{1}H magnetic resonance (MR)-type switching probes have been reported as powerful tools for in vivo enzyme imaging by Meade's group.[4a] The switching mechanisms are mainly based on paramagnetic relaxation enhancement (PRE) using paramagnetic metal complexes and their coordinated water molecules.[5] For target-specific imaging, heteronuclear MRI techniques have also attracted considerable attention. In particular, ^{19}F MRI is anticipated to be a promising method because ^{19}F has a high NMR sensitivity approaching that of ^{1}H (83% relative to ^{1}H) and there are no background signals even in vivo.[6] Despite the potential importance of ^{19}F MRI for medical diagnostics, promising strategies for imaging specific enzymes with high contrast are as yet very limited.[7] There are also some problems associated with ^{19}F MRI that have yet to be overcome, namely low sensitivity and poor efficiency of probe delivery. Therefore, ^{19}F MRI is an immature technique and both more fundamental studies on ^{19}F probes and improvement of the instrumentation are needed to establish it as an in vivo imaging tool.

Recently, we have developed a unique self-assembling turn-on ^{19}F probe for the specific detection of target proteins composed of a hydrophilic protein ligand and a hydrophobic ^{19}F detection modality.[8] These ligand-tethered probes clearly exhibit a disassembly driven turn-on signal change upon specific binding to target proteins.[8,9] More recently, we have established that moderate stability of the aggregates is critical for obtaining an ideal off/on response, and the stability can be controlled by the hydrophobicity/hy-

[a] K. Matsuo, Dr. R. Kamada, Dr. K. Mizusawa, Dr. Y. Takaoka, Prof. Dr. I. Hamachi
Department of Synthetic Chemistry and Biological Chemistry
Graduate School of Engineering, Kyoto University
Katsura, Nishikyo-Ku, Kyoto 615-8510 (Japan)
Fax: (+81) 75-383-2759
E-mail: ihamachi@sbchem.kyoto-u.ac.jp

[b] Dr. H. Imai, Dr. Y. Takayama, Dr. M. Narazaki, Prof. Dr. T. Matsuda
Department of System Science, Graduate School of Informatics
Kyoto University, 361-1 Yoshida-Honmachi
Sakyo-ku, Kyoto 606-8501 (Japan)

[c] Prof. Dr. I. Hamachi
Japan Science and Technology Agency (JST), CREST
5 Sanbancho, Chiyoda-ku, Tokyo 102-0075 (Japan)

Supporting information for this article is available on the WWW under http://dx.doi.org/10.1002/chem.201300817.

drophilicity balance of the probe.[10] However, since this turn-on sensing requires 1:1 complex formation between a ligand and a protein, its sensitivity is inherently limited to the concentration of the target protein. This seemed to be a critical disadvantage, especially in the case of ^{19}F MR probes, which typically only have sensitivity down to the micromolar level.

Herein, we describe novel self-assembling ^{19}F probes showing signal-amplification properties for the specific and highly sensitive detection and imaging of enzyme activities (Scheme 1). These probes employ a "substrate" for the target enzyme instead of a ligand for a protein, and the signals can be amplified by the catalytic enzyme reaction.

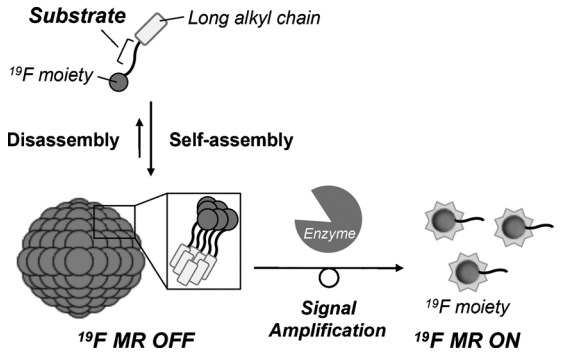

Scheme 1. Schematic illustration of a substrate-based self-assembling ^{19}F probe for turn-on detection of enzymatic activity.

Using these new self-assembling ^{19}F probes, detection and imaging of two different enzymes, nitroreductase (NTR) and matrix metalloproteinase (MMP), at the nanomolar level has been accomplished by ^{19}F NMR spectroscopy and MRI. Furthermore, we have succeeded in the turn-on imaging of the activity of MMP endogenously secreted in the cultured media of tumor cells by the ^{19}F MRI phantom technique, which clearly demonstrated that our substrate-based turn-on probes are capable of serving as a platform for screening the MMP activities of several mammalian cell lines.

Results and Discussion

Substrate-based ^{19}F MRI probes for turn-on detection of nitroreductase activity: As proof-of-principle experiments, we initially employed nitroreductase (NTR) as a target enzyme.[11] According to guidelines established by our previous ligand-tethered probes, a new ^{19}F probe **1** was designed with the ability to self-assemble, composed of a hydrophobic alkyl chain appended *para*-nitrobenzene as a substrate moiety for NTR, and a hydrophilic ^{19}F-containing detection moiety. This ^{19}F moiety (3,5-bis(trifluoromethyl)benzene (FB)-appended aspartate; compound **2**) was linked to *para*-nitrobenzene through a carbonate ester bond.[12] This "substrate-based probe" alone is "NMR-silent" because of its self-assembly, but should give a distinct ^{19}F signal from the monomeric FB unit produced upon its cleavage triggered by nitro group reduction with NTR (Figure 1a).

To test the turn-on property of probe **1**, we initially monitored the ^{19}F NMR spectra with or without NTR. When **1** (50 μM) was dissolved in a buffer solution, no ^{19}F NMR signal was observed. In contrast, a sharp signal appeared at $\delta = -62.9$ ppm upon addition of NTR (0.83 μM) and incubation for 60 min at 37 °C (Figure 1b). This new signal could be assigned to compound **2** by ^{19}F NMR and HPLC analyses (Figure S1 in the Supporting Information), which was produced by an NTR-catalyzed tandem reaction. These results clearly showed that nitro group reduction followed by β-1,6-elimination indeed occurred in the presence of NTR, resulting in the turn-on signal change. Probe **1** alone showed relatively high light scattering at 600 nm (O.D. 600, Figure 1c) in a buffer solution. Dynamic light-scattering (DLS) measurements of **1** alone also showed aggregates with a mean diameter of 100 nm (Figure 1d), whereas negligible scattering intensity was observed after 60 min incubation with NTR. These results indicated that the enzymatic reaction induced destruction of the aggregates. Thus, it is clear that **1** can serve as an off/on-type probe driven by enzymatic reaction-triggered disassembly. Furthermore, probe **1** allowed us to visualize the enzymatic activity in a ^{19}F MRI phantom technique owing to its ideal off/on response, as shown in Figure 1e.

Development of an MMP2 substrate-based ^{19}F probe and detection of MMP2 activity in a test tube: Benefiting from the modular design of our self-assembling probes, a new substrate-based probe was readily extended to detection of the activities of other enzymes. Matrix metalloproteinase 2 (MMP2), a target enzyme of our next substrate-based self-assembling probe, is a protease secreted from cell membranes and is involved in cell migration and remodeling processes through its degradation action on the extracellular matrix.[13] MMP2 and MMP9 are also related to tumor invasion, metastasis, and angiogenesis, making them valuable targets for cancer diagnosis and treatment. Similar to the NTR probe, an off/on-type ^{19}F probe, **3a**, containing a hydrophilic MMP2 substrate peptide (GPLG-VRG) was designed and synthesized (see Scheme 2).[14] In this probe, a hydrophobic dodecyl chain (C12) is attached to the N-terminus of the substrate through a tetraethyleneglycol linker (O4 linker), and FB is tethered to the substrate through an additionally incorporated lysine at the C-terminus (Figure 2a). Upon cleavage by MMP2, a hydrophilic peptide containing FB (VRGK(FB), compound **5**) is expected to be produced, which should give a clear ^{19}F NMR signal.

Firstly, it was confirmed that probe **3a** alone (50 μM) showed no ^{19}F NMR signal in a buffer solution. We then found that a sharp signal appeared at $\delta = -62.9$ ppm upon addition of MMP2 (15 nM) and incubation for 24 h at 37 °C (Figure 2b and Figure S2 in the Supporting Information). In contrast, no ^{19}F signal recovery was observed after incubation of probe **3a** with MMP2 in the presence of an MMP2 inhibitor (compound **6**, 100 μM, Figure 2c).[15] Probe **7**, in

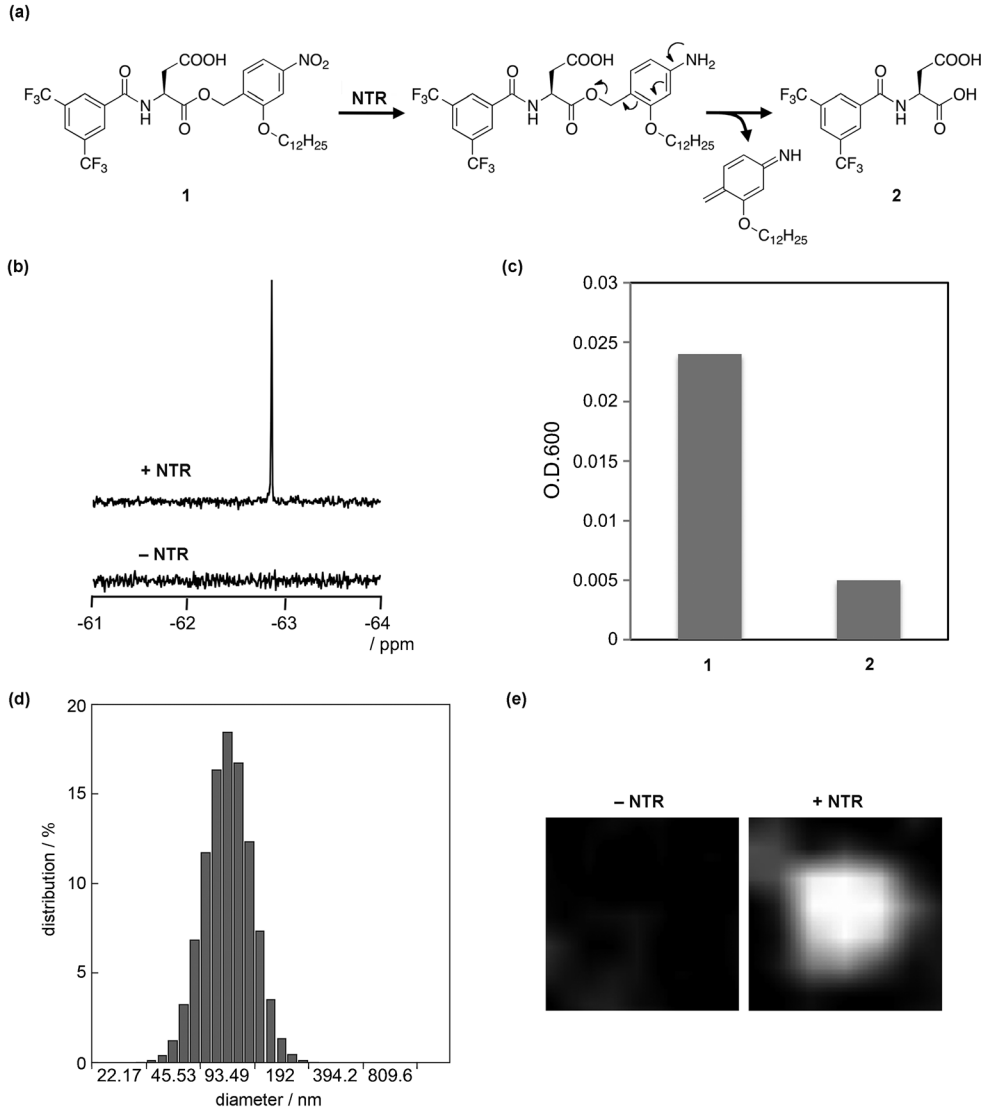

Figure 1. Substrate-based turn-on ^{19}F probe for detection of nitroreductase activity. a) Chemical structure of probe **1**, and proposed reduction and ensuing elimination mechanism with NTR. b) ^{19}F NMR spectra of probe **1** in the absence of NTR (bottom) and after incubation with NTR (0.83 μM) at 37 °C for 60 min (top). c) Optical densities of probe **1** (50 μM, left) and compound **2** (50 μM, right). d) DLS analysis of the particle-size distribution of probe **1** (50 μM). e) ^{19}F MR images of probe **1** in the absence of NTR (left) and after incubation with NTR (0.83 μM) at 37 °C for 60 min (right). All experiments illustrated in this figure were performed in 50 mM 2-[4-(2-hydroxyethyl)piperazin-1-yl]ethanesulfonic acid (HEPES) buffer (pH 7.2, containing nicotinamide adenine dinucleotide phosphate (NADPH; 1.0 mM), D_2O (10 %), and trifluoroacetic acid (TFA; 0.1 mM) as an internal standard ($\delta = -75.6$ ppm)).

which we replaced the substrate part with a nonsubstrate peptide (GVRLGPG), also gave no response with MMP2 (Figure S3 in the Supporting Information).[14a] Given these results, we demonstrated that an ideal turn-on ^{19}F probe for the specific detection of MMP2 activity could be successfully prepared in a test tube. More importantly, the detection limit of MMP2 with probe **3a** was found to be less than 0.5 nM (Figure 2d and Figure S4 in the Supporting Information), which is at least 10000-fold lower than those of our previous ligand-tethered probes (i.e., 5 μM in the case of a benzenesulfonamide-appended ^{19}F probe for the detection of human carbonic anhydrase I).[8a]

Examination of the self-assembling properties and MMP2 response of the MMP2-substrate-based ^{19}F probes: Next, we investigated the self-assembling properties of the MMP2-type ^{19}F probes, in order to explore the response mechanism in detail. Fluorescent microscopy of aggregates of **3a** loaded with Nile Red showed spherical shapes with diameters ranging from 0.5 to 1 μm (Figure 3a).[16] From DLS measurements, a buffer solution containing **3a** alone showed aggregates with a mean diameter of 600 nm (Figure 3b), whereas negligible scattering intensity was detected upon cleavage by MMP2. Aggregation of **3a** resulted in a dramatic increase in the apparent molecular mass (M_r) from 1.5×10^3 (monomer) to 7×10^7 Da. It is reasonable that such an increase in M_r caused a significant increase in the ^{19}F relaxa-

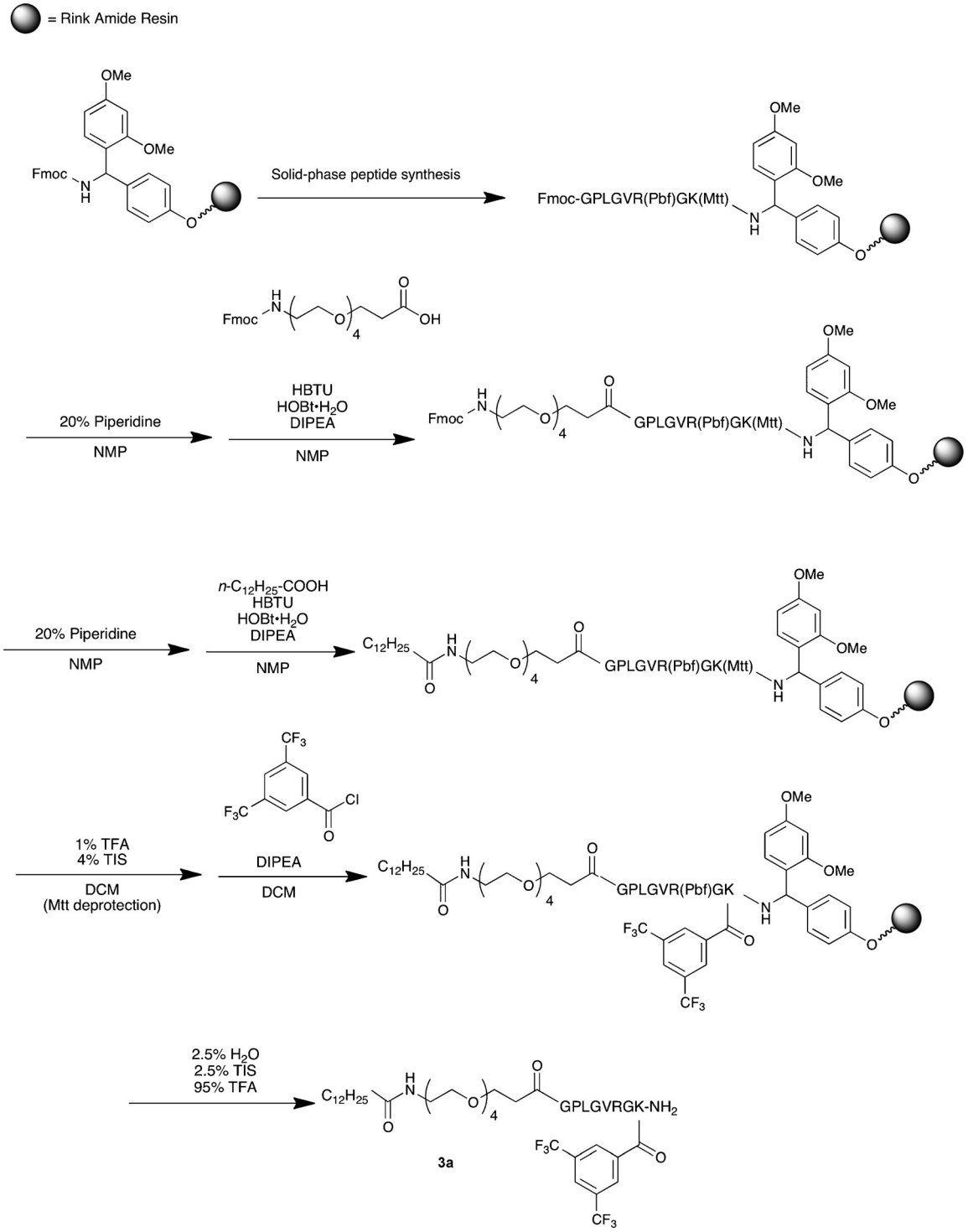

Scheme 2. Synthetic route to probe **3a**.

tion rate, affording no NMR signals, as in the case of our previous ligand-tethered ^{19}F probes.[8]

In our previous study, we clarified that the stability of the aggregates of the ligand-tethered probes was critical for their off/on response.[10] In order to examine the relationship between the aggregation property and reactivity of the substrate-based probes, we additionally prepared two further ^{19}F probes **3b** and **3c**. Compound **3a** has a tetraethyleneglycol (O4) linker between the hydrophobic alkyl chain and the N-terminus of the substrate, whereas **3b** has no linker and **3c** has a diethyleneglycol (O2) linker (Figure 2a). These two probes alone showed no ^{19}F NMR signals in buffer solutions, indicating that they both formed self-assembled aggregates like probe **3a**. The critical aggregation

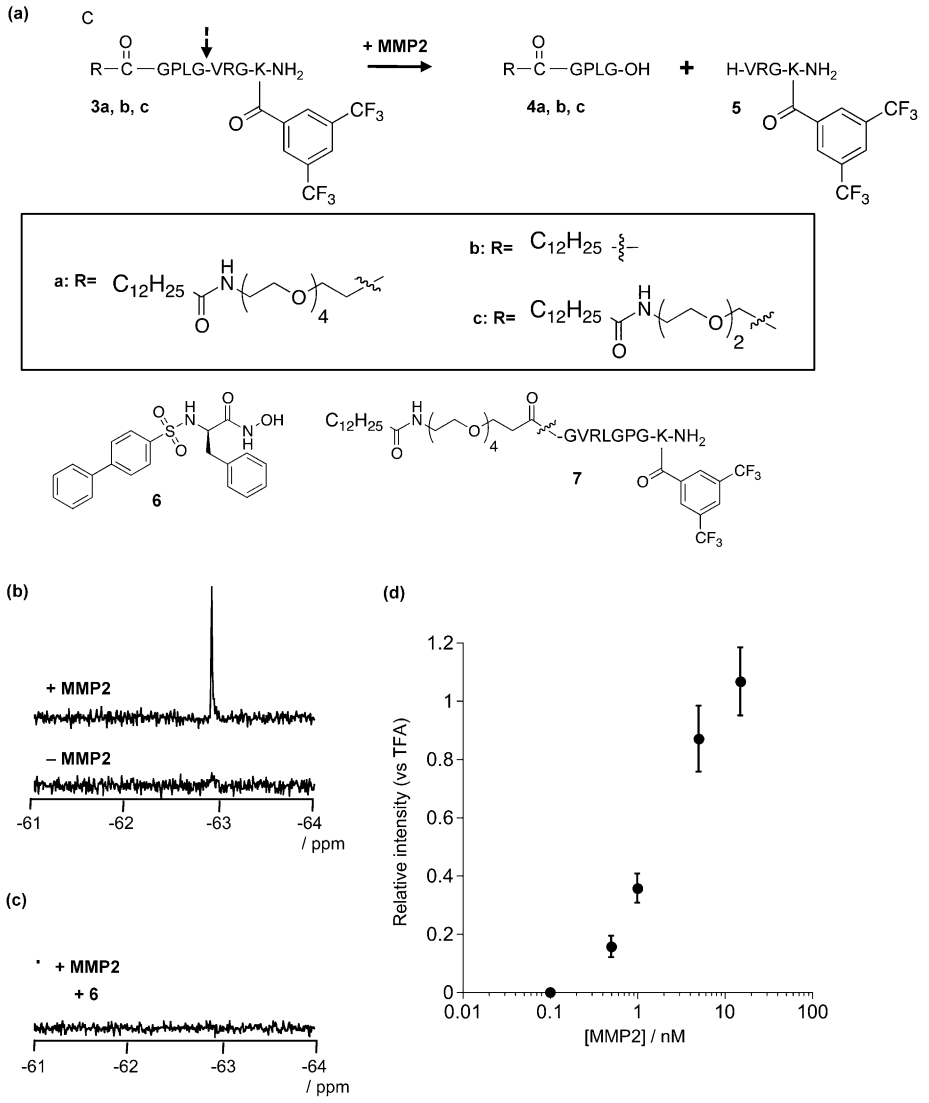

Figure 2. Substrate-based turn-on ^{19}F probes for the detection of matrix metalloproteinase-2 (MMP2) activity. a) Chemical structures of probes **3a–c**, **7**, cleaved compounds **4a–c**, **5**, and MMP2 inhibitor **6**. b) ^{19}F NMR spectra of probe **3a** (100 μM) in the absence of MMP2 (bottom) and after incubation with MMP2 (15 nM) at 37 °C for 24 h (top). c) ^{19}F NMR spectrum of probe **3a** (100 μM) in the presence of MMP2 (15 nM) and inhibitor **6** (100 μM). d) Semi-log plot of relative ^{19}F NMR signal intensity versus MMP2 concentration. Error bars represent standard deviations of three experiments (the respective ^{19}F NMR spectra are shown in Figure S4 in the Supporting Information). All experiments illustrated in this figure were performed in 50 mM HEPES buffer (pH 7.5 containing NaCl (100 mM), $CaCl_2$ (10 mM), D_2O (10 %), and TFA (0.1 mM) as an internal standard, $\delta = -75.6$ ppm).

concentration (CAC) values of all three probes (**3a**, **3b**, and **3c**) were about 5 μM (Figure 3c).[16] The CAC values of compounds **4a** and **5** (the two products from probe **3a** hydrolyzed by MMP2, as shown in Figure 2a), on the other hand, were higher than 100 μM, which clearly indicated that the self-assembled aggregates of **3a** collapsed due to the MMP2 enzymatic reaction under the present conditions. Interestingly, the initial rates of ^{19}F NMR signal recovery were different among probes **3a**, **3b**, and **3c**, specifically 20, 7.5, and 15 μM h^{-1}, respectively (Figure 3d). These findings suggested that the flexibility of the linker moiety is critical for the efficient access of MMP2 so as to result in a rapid response of these substrate probes. The k_{cat} value for MMP2 determined by using the ideal off/on-type probe **3a** was in good agreement with that reported by using a monodisperse MMP2 substrate (Table 1 and Figure S5 in the Supporting Information).[17]

Detection and imaging of MMP activity in MMP-secreted cultured media from tumor cells: With the substrate-based turn-on ^{19}F probe **3a** for MMP2 in hand, we finally applied it for the detection of MMP activity in a medium of cultured tumor cells. HT-1080 cells, a model cell line secreting MMP2 or MMP9,[18] were cultured without serum for 48 h and then the supernatant was collected. The supernatant was mixed with 50 μM probe **3a**, and then incubated for 24 h in the absence or presence of MMP2 inhibitor (compound **6**, 100 μM). A sharp ^{19}F NMR signal appeared in the absence of the inhibitor **6**, whereas no signal was detected in its presence (Figure 4a,b). ^{19}F MRI phantom experiments by using this turn-on probe (**3a**) allowed us to visualize the MMP activity with a high signal-to-noise ratio.[19] As shown in Figure 4c, a clear ^{19}F MR image was observed for the supernatant of HT-1080 cells, whereas no clear ^{19}F MR image was obtained in the presence of inhibitor **6**.[20] Figure 4d shows the dependence of con-

Table 1. Kinetic parameters of purified MMP2 for the hydrolysis of a self-assembling ^{19}F probe and monodispersed-type peptide.

Substrate derivatives	Kinetic parameters k_{cat} [s^{-1}]	$1/K_m$ [M^{-1}]	k_{cat}/K_m [s^{-1} M^{-1}]
Probe **3a**[a]	3.9	1.6×10^4	6.3×10^4
Ac-PLGVRG-OC_2H_5	4.1	3.4×10^3	1.4×10^4

[a] These values were determined fluorometrically according to a previous report by using fluorescamine to label the amino terminal groups created by peptide bond cleavage.[17]

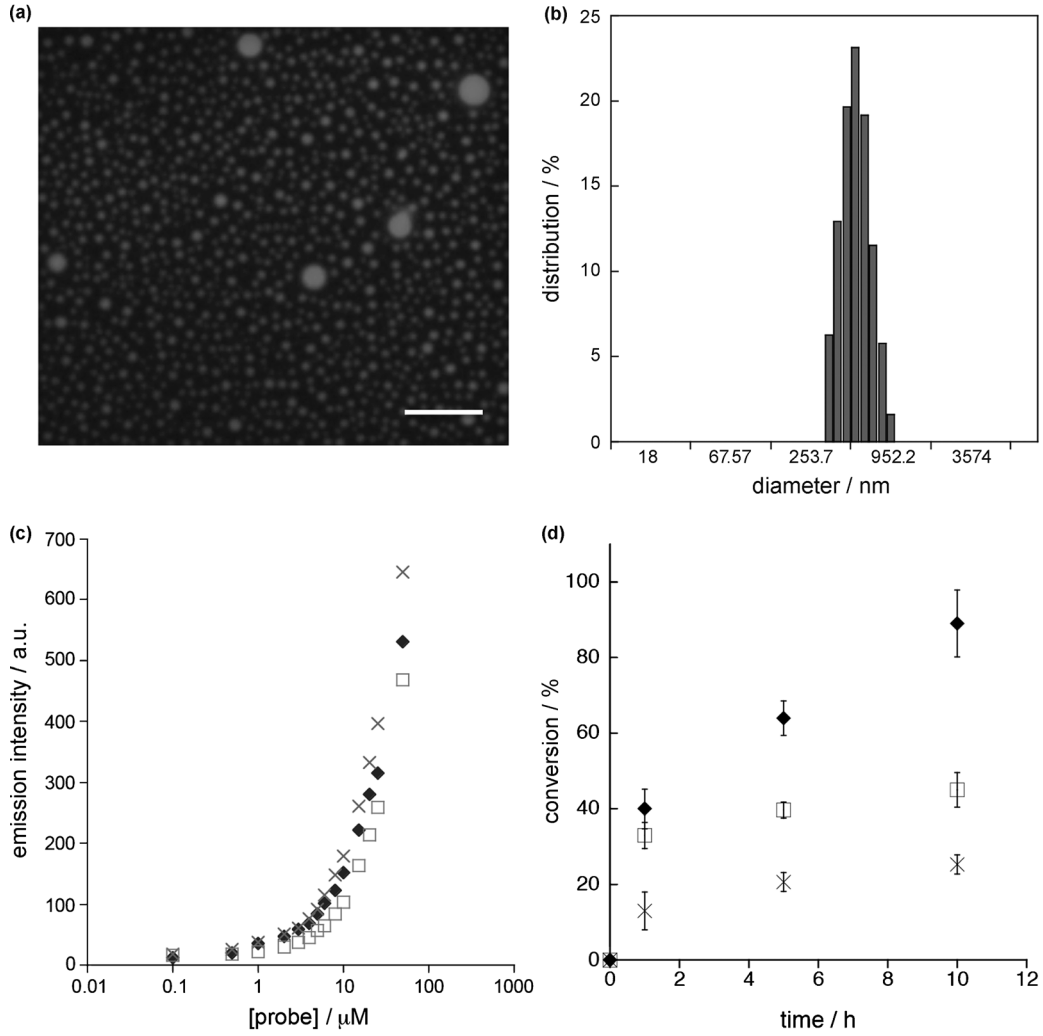

Figure 3. a, b) Self-assembling properties of MMP2-type probe **3a**. a) Fluorescent microscopy image of probe **3a** (50 μM) loaded with Nile Red (5 μM). Scale bar 5 μm. b) DLS analysis of the particle-size distribution of probe **3a** (50 μM). c) Fluorescent intensity changes of Nile Red (5 μM) with the addition of probe **3a** (◆), **3b** (×), or **3c** (□ (λ_{em} = 575 nm). d) Time profiles of hydrolysis reactions of probes **3a** (◆), **3b** (×), and **3c** (□) with MMP2. All experiments illustrated in this figure were performed in 50 mM HEPES buffer (pH 7.5 containing NaCl (100 mM), $CaCl_2$ (10 mM), D_2O (10%), and TFA (0.1 mM)).

trast on the number of scans accumulated, and the contrast was distinctly higher with increasing number of accumulations. An image with sufficient contrast was nevertheless successfully obtained after just 900 accumulations (about 15 min).

Similarly, well-defined ^{19}F NMR/MRI signals were observed for HeLa cells, which have previously been reported to be an MMP2-secreting cell line (Figure 4e and Figure S7 in the Supporting Information).[21] In contrast, no signals were detected for Jurkat[22] or COS7 cells,[23] two non-MMP2-secreting cell lines. Therefore, it is clear that our self-assembling ^{19}F probe for imaging of enzymatic activity may serve as a screening platform for the activity of MMPs. More interestingly, in the case of human breast cancer MCF7 cells, distinct ^{19}F NMR and MR signals were only observed when the cells were cultured under conditions of hypoxia, and not under normoxia (Figure 4f). Similarly, by treatment of MCF7 cells with antimycin A or rotenone, a sharp ^{19}F NMR signal appeared (Figure S8 in the Supporting Information). It has recently been reported that conditions of hypoxia or addition of these compounds can induce or promote MMP2 secretion in live MCF7 cells by producing reactive oxygen species (ROS).[24] The present results demonstrate that the turn-on ^{19}F probes may potentially be useful for visualizing drug-triggered enzyme induction in live tumor cells.

Conclusion

We have developed new signal-amplifiable self-assembling ^{19}F NMR/MRI probes for the sensitive detection and imaging of specific enzymatic activity. The simple principle for the off/on response (that is, self-assembly and enzymatic

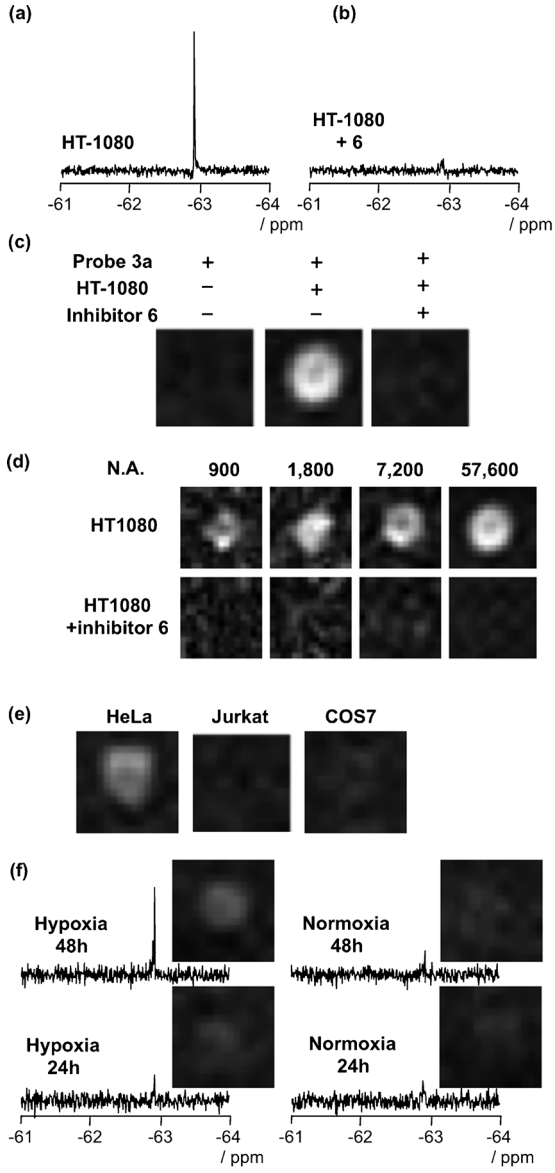

Figure 4. a, b) ^{19}F NMR spectra of probe **3a** (50 μM) in the supernatant of HT-1080 cells in the a) absence or b) presence of inhibitor **6** (100 μM). The samples were reacted at 37 °C for 48 h in the cultured media (collected from 48 h pre-incubated cells without serum, including D_2O (10%) and TFA (0.1 mM) as an internal standard). c) ^{19}F MR images of probe **3a** (50 μM) in the supernatant of HT-1080 cells in the absence or presence of inhibitor **6** (100 μM). The samples were incubated at 37 °C for 48 h in each cultured medium (collected from 48 h pre-incubated cells without serum, including D_2O (10%) and TFA (0.1 mM) as an internal standard). d) ^{19}F MR images of probe **3a** (50 μM) in the supernatant of HT-1080 cells in the absence (top) or presence (bottom) of inhibitor **6** (100 μM) with different number of accumulation (N.A.). e) ^{19}F MR images of probe **3a** in the supernatants of various cell lines (HeLa, Jurkat, and COS7 cells). The samples were incubated at 37 °C for 48 h in each cultured medium (collected from 48 h pre-incubated cells without serum, including D_2O (10%) and TFA (0.1 mM) as an internal standard). f) ^{19}F NMR spectra and MR images of probe **3a** in the supernatants of MCF7 cells cultured under the indicated conditions. The samples were incubated at 37 °C for 48 h in the cultured media (collected from pre-incubated cells under hypoxia or normoxia conditions (24 and 48 h pre-incubation), including D_2O (10%) and TFA (0.1 mM) as an internal standard).

cleavage-triggered disassembly of the probe) should be applicable for various target enzymes by appropriately replacing the substrate module, as shown here for two different enzymes (NTR and MMP2). The detection limit of these substrate-based probes was found to be less than 0.5 nM, which is at least 10000-fold lower than that of our previous ligand-tethered ^{19}F probes. Moreover, by using our novel substrate-based self-assembling probe, we succeeded in imaging the activity of endogenously secreted matrix metalloproteinase (MMP, a valuable target for cancer diagnosis and treatment) in the media of tumor cells by ^{19}F MRI phantom techniques, depending on the cell lines and the cellular conditions. From a practical viewpoint, it may be fair to say that the sensitivity of ^{19}F is considerably lower than that of conventionally used Gd-based ^{1}H MRI probes. However, further advances in both instrumentation and chemistry (e.g., increasing the number of equivalents of fluorine in the probe for higher sensitivity) may overcome this limitation, and the ^{19}F NMR/MRI technique may become a more powerful modality for target-specific in vivo imaging. We believe that employing our self-assembling turn-on ^{19}F probe for monitoring enzyme activities should facilitate the use of ^{19}F MRI techniques in cells and in vivo.

Experimental Section

General materials and methods: All proteins and chemicals were obtained from commercial suppliers (Aldrich, Tokyo Chemical Industry (TCI), Wako Pure Chemical Industries, Sasaki Chemical, Watanabe Chemical Industries, Calbiochem) and were used without further purification. Thin-layer chromatography (TLC) was performed on silica gel 60 F_{254} precoated aluminum sheets (Merck) and spots were visualized by fluorescence quenching or ninhydrin staining. Chromatographic purifications were conducted by flash column chromatography on silica gel 60 N (neutral, 40–50 μm, Kanto Chemical). ^{1}H NMR spectra were recorded from solutions in deuterated solvents on a Varian Mercury 400 (400 MHz) spectrometer and calibrated to the residual solvent peak or tetramethylsilane ($\delta = 0$ ppm). Multiplicities are abbreviated as follows: s = singlet, d = doublet, t = triplet, q = quartet, quin = quintet, m = multiplet, dd = doublet of doublets. ^{19}F NMR spectra were recorded on a JEOL ECX-400P (376.5 MHz) spectrometer and calibrated with TFA ($\delta = -75.6$ ppm). Standard parameters were used: spectral width 36 kHz, pulse length 8 μs, acquisition time 0.46 s, and relaxation delay 0.50 s. A 0.1 Hz line broadening was applied. The number of accumulations was 1024. ^{19}F MR images were obtained on a 7 T Bruker-Biospec 70/20 USR system (282 MHz for ^{19}F) with 72 mm i.d. ^{1}H/^{19}F radiofrequency (RF) volume coil (Bruker Biospin, Germany). UV/Vis spectra were recorded on a Shimadzu UV-2550 spectrometer. DLS measurements were performed with a NICOMP 380zls apparatus (wavelength of the laser 520 nm). Matrix-assisted laser desorption/ionization time-of-flight mass spectrometry (MALDI-TOF MS) was performed on an Autoflex II instrument (Bruker Daltonics) by using α-cyano-4-hydroxycinnamic acid (CHCA) as the matrix. High-resolution electrospray ionization quadrupole Fourier-transform mass spectroscopy (HR-ESI Qq-LTMS) was carried out on a Bruker Apex-Ultra (7 T) mass spectrometer. HPLC purification was conducted with a Lachrom chromatograph (Hitachi, Japan).

Synthesis: Synthetic procedures and compound characterizations are mainly described in the Supporting Information. Probe **3a** was synthesized manually on Rink amide resin (Novabiochem) by a standard Fmoc-based solid-phase peptide synthesis protocol (Scheme 2). Fmoc-Gly-OH, Fmoc-Pro-OH, Fmoc-Leu-OH, Fmoc-Val-OH, Fmoc-Arg(Pbf)-OH, and Fmoc-Lys(Mtt)-OH were used as building blocks (Pbf: 2,2,4,6,7-pentame-

thyldihydrobenzofurane-5-sulfonyl; Mtt: 4-methyltrityl; Fmoc = fluorenylmethyloxycarbonyl). Fmoc deprotection was performed with 20% piperidine in *N*-methylpyrrolidone (NMP); Mtt deprotection was performed in dichloromethane containing 1% TFA and 4% triisopropylsilane (TIS). Coupling reactions were performed with a mixture of Fmoc-amino acid (3 equiv), *O*-benzotriazole-*N*,*N*,*N*′,*N*′-tetramethyluronium hexafluorophosphate (HBTU; 3 equiv), 1-hydroxybenzotriazole hydrate ($HOBt{\cdot}H_2O$; 3 equiv), and diisopropylethylamine (DIPEA; 6 equiv) in NMP at room temperature. All coupling and Fmoc/Mtt deprotection steps were monitored by the Kaiser test. Following chain assembly, global deprotection and cleavage from the resin was performed with TFA containing 2.5% TIS and 2.5% H_2O. The crude peptide products were precipitated by the addition of diethyl ether and purified by reversed-phase HPLC (eluent: A (acetonitrile containing 0.1% TFA)/B (0.1% aq. TFA) = 20:80 (0 min)→20:80 (10 min) → 90:10 (45 min)). The obtained compound was lyophilized, and the residue was dissolved in 5% hydrogen chloride/methanol reagent (TCI). The solution was concentrated and the residue was dried in vacuo to yield **3a** as the hydrogen chloride salt. Probe **3a** was characterized by reversed-phase HPLC (Figure S9 in the Supporting Information) and MALDI-TOF MS (calcd for $[M+H]^+$: 1465.83; found: 1465.55).

Cell culture: HT-1080, HeLa, COS7, and MCF7 cells were cultured in high-glucose Dulbecco's Modified Eagle Medium (DMEM, 4.5 g of glucose L^{-1}) supplemented with 10% fetal bovine serum (FBS), penicillin (100 units mL^{-1}), and streptomycin (100 μg mL^{-1}) under a humidified atmosphere of 5% CO_2 in air. Jurkat cells were cultured in RPMI-1640 medium supplemented with 10% FBS, penicillin (100 units mL^{-1}), and streptomycin (100 μg mL^{-1}). For all experiments, cells were harvested from subconfluent (<80%) cultures by using a trypsin/ethylenediaminetetraacetic acid (EDTA) solution and then resuspended in fresh medium. A subculture was performed every 2–3 days.

^{19}F NMR/MR images of probe 3a in the supernatants of various cells: All cells were plated at a density of 5.0×10^6 cells per 60 mm dish and cultured for 24 h at 37 °C in air with 5% CO_2. The cells (except for MCF7 cells) were washed three times, and cultured in serum-free DMEM or RPMI-1640 for 24 h. The MCF7 cells were washed three times, and cultured in serum-free DMEM for 12, 24, or 48 h at 37 °C under normoxic conditions (air with 5% CO_2) or hypoxic conditions (<0.1% O_2) generated with an AnaeroPack (Mitsubishi Gas Chemical Company, Inc.) and a rectangular jar. The conditioned media were then collected and centrifuged, and probes were added to give a final concentration of 50 μM. After incubation for 48 h at 37 °C, magnetic resonance measurements were conducted as follows. In ^{19}F NMR experiments, samples (conditioned medium) of 450 μL were added to 50 μL of D_2O containing TFA (final concentration 100 μM). ^{19}F NMR spectra were then measured at 20 °C. In ^{19}F MR imaging experiments, aliquots of conditioned medium (2 mL) were loaded into sample tubes (depth of each sample tube 20 mm). ^{19}F MR images of samples were obtained by fast spin echo with a repetition time/echo time of 1000/5.5 ms, an echo train length of 32, a field of view of 32×8 cm^2 without slice selection, a matrix size of 128×32, and 57600 accumulations. The excitation pulse width was 1370 Hz. Zero-filling (256×64) was applied to the ^{19}F MR images. All images were acquired at 20 °C.

Acknowledgements

Prof. K. Matsuda (Kyoto University) is acknowledged for his help with the DLS measurements. K.M. acknowledges the JSPS Research Fellowships for Young Scientists. This work is partly supported by the Innovative Techno-Hub for Integrated Medical Bio-imaging of the Project for Developing Innovation Systems, from the Ministry of Education, Culture, Sports, Science and Technology (MEXT), Japan and by the Japan Science and Technology Agency (CREST).

[1] a) R. Weissleder, U. Mahmood, *Radiology* **2001**, *219*, 316; b) R. Weissleder, M. J. Pittet, *Nature* **2008**, *452*, 580; c) J. V. Frangioni, *Curr. Opin. Chem. Biol.* **2003**, *7*, 626.

[2] a) L. D. Lavis, R. T. Raines, *ACS Chem. Biol.* **2008**, *3*, 142; b) H. Kobayashi, M. Ogawa, R. Alford, P. L. Choyke, Y. Urano, *Chem. Rev.* **2010**, *110*, 2620.

[3] a) G. Zlokarnik, P. A. Negulescu, T. E. Knapp, L. Mere, N. Burres, L. Feng, M. Whitney, K. Roemer, R. Y. Tsien, *Science* **1998**, *279*, 84; b) W. Gao, B. Xing, R. Y. Tsien, J. Rao, *J. Am. Chem. Soc.* **2003**, *125*, 11146; c) M. Kamiya, H. Kobayashi, Y. Hama, Y. Koyama, M. Bernardo, T. Nagano, P. L. Choyke, Y. Urano, *J. Am. Chem. Soc.* **2007**, *129*, 3918; d) S. Mizukami, K. Kikuchi, T. Higuchi, Y. Urano, T. Mashima, T. Tsuruo, T. Nagano, *FEBS Lett.* **1999**, *453*, 356.

[4] a) A. Y. Louie, M. M. Hüber, E. T. Ahrens, U. Rothbächer, R. Moats, R. E. Jacobs, S. E. Fraser, T. J. Meade, *Nat. Biotechnol.* **2000**, *18*, 321; b) J. M. Perez, L. Josephson, T. O'Loughlin, D. Högemann, R. Weissleder, *Nat. Biotechnol.* **2002**, *20*, 816; c) F. Kiessling, B. Morgenstern, C. Zhang, *Curr. Med. Chem.* **2007**, *14*, 77; d) D. E. Sosnovik, R. Weissleder, *Curr. Opin. Biotechnol.* **2007**, *18*, 4.

[5] a) R. B. Lauffer, *Chem. Rev.* **1987**, *87*, 901; b) S. Zhang, W. Kuangcong, A. D. Sherry, *Angew. Chem.* **1999**, *111*, 3382; *Angew. Chem. Int. Ed.* **1999**, *38*, 3192; c) W. Li, S. E. Fraser, T. J. Meade, *J. Am. Chem. Soc.* **1999**, *121*, 1413; d) B. Yoo, M. D. Pagel, *J. Am. Chem. Soc.* **2006**, *128*, 14032.

[6] a) M. Higuchi, N. Iwata, Y. Matsuba, K. Sato, K. Sasamoto, T. C. Saido, *Nat. Neurosci.* **2005**, *8*, 527; b) D. Zhao, L. Jiang, R. P. Mason, *Methods Enzymol.* **2004**, *386*, 378; c) E. T. Ahrens, R. Flores, H. Xu, P. A. Morel, *Nat. Biotechnol.* **2005**, *23*, 983; d) J.-X. Yu, R. R. Hallac, S. Chiguru, R. P. Mason, *Prog. Nucl. Magn. Reson. Spectrosc.* **2013**, *70*, 25.

[7] a) W. Cui, P. Otten, Y. Li, K. S. Koeneman, J. Yu, R. P. Mason, *Magn. Reson. Med.* **2004**, *51*, 616; b) K. Tanabe, H. Harada, M. Narazaki, K. Tanaka, K. Inafuku, H. Komatsu, T. Ito, H. Yamada, Y. Chujo, T. Matsuda, M. Hiraoka, S. Nishimoto, *J. Am. Chem. Soc.* **2009**, *131*, 15982; c) K. Yamaguchi, R. Ueki, H. Nonaka, F. Sugihara, T. Matsuda, S. Sando, *J. Am. Chem. Soc.* **2011**, *133*, 14208; d) L. D. Stegman, A. Rehemtulla, B. Beattie, E. Kievit, T. S. Lawrence, R. G. Blasberg, J. G. Tjuvajev, B. D. Ross, *Proc. Natl. Acad. Sci. USA* **1999**, *96*, 9821; e) S. Mizukami, R. Takikawa, F. Sugihara, Y. Hori, H. Tochio, M. Wälchli, M. Shirakawa, K. Kikuchi, *J. Am. Chem. Soc.* **2008**, *130*, 794; f) A. Keliris, I. Mamedov, G. E. Hagberg, N. K. Logothetis, K. Scheffler, J. Engelmann, *Contrast Media Mol. Imaging* **2012**, *7*, 478; g) K. Tanaka, N. Kitamura, K. Naka, Y. Chujo, *Chem. Commun.* **2008**, 6176.

[8] a) Y. Takaoka, T. Sakamoto, S. Tsukiji, M. Narazaki, T. Matsuda, H. Tochio, M. Shirakawa, I. Hamachi, *Nat. Chem.* **2009**, *1*, 557; b) Y. Takaoka, Y. Sun, S. Tsukiji, I. Hamachi, *Chem. Sci.* **2011**, *2*, 511.

[9] a) K. Mizusawa, Y. Ishida, Y. Takaoka, M. Miyagawa, S. Tsukiji, I. Hamachi, *J. Am. Chem. Soc.* **2010**, *132*, 7291; b) K. Mizusawa, Y. Takaoka, I. Hamachi, *J. Am. Chem. Soc.* **2012**, *134*, 13386.

[10] Y. Takaoka, K. Kiminami, K. Mizusawa, K. Matsuo, M. Narazaki, T. Matsuda, I. Hamachi, *J. Am. Chem. Soc.* **2011**, *133*, 11725.

[11] a) S. Zenno, H. Koike, A. N. Kumar, R. Jayaraman, M. Tanokura, K. Saigo, *J. Bacteriol.* **1996**, *178*, 4508; b) M. D. Roldán, E. Pérez-Reinado, F. Castillo, C. Moreno-Vivián, *FEMS Microbiol. Rev.* **2008**, *32*, 474.

[12] a) E. Nakata, Y. Yukimachi, H. Kariyazono, S. Im, C. Abe, Y. Uto, H. Maezawa, T. Hashimoto, Y. Okamoto, H. Hori, *Bioorg. Med. Chem.* **2009**, *17*, 6952; b) L. Cui, Y. Zhong, W. Zhu, Y. Xu, Q. Du, X. Wang, X. Qian, Y. Xiao, *Org. Lett.* **2011**, *13*, 928; c) Y. Chen, L. Hu, *Med. Res. Rev.* **2009**, *29*, 29.

[13] a) A. Page-McCaw, A. J. Ewald, Z. Werb, *Nat. Rev. Mol. Cell Biol.* **2007**, *8*, 221; b) C. Gialeli, A. D. Theocharis, N. K. Karamanos, *FEBS J.* **2011**, *278*, 16.

[14] a) C. Bremer, C.-H. Tung, R. Weissleder, *Nat. Med.* **2001**, *7*, 743; b) C. Bremer, S. Bredow, U. Mahmood, R. Weissleder, C.-H. Tung, *Radiology* **2001**, *221*, 523; c) J. Deguchi, M. Aikawa, C.-H. Tung, E. Aikawa, D.-E. Kim, V. Ntziachristos, R. Weissleder, P. Libby, *Circu-*

lation **2006**, *114*, 55; d) S. Lee, E.-J. Cha, K. Park, S.-Y. Lee, J.-K. Hong, I.-C. Sun, S. Y. Kim, K. Choi, I. C. Kwon, K. Kim, C.-H. Ahn, *Angew. Chem.* **2008**, *120*, 2846; *Angew. Chem. Int. Ed.* **2008**, *47*, 2804; e) T. Myochin, K. Hanaoka, T. Komatsu, T. Terai, T. Nagano, *J. Am. Chem. Soc.* **2012**, *134*, 13730; f) M. Zhao, L. Josephson, Y. Tang, R. Weissleder, *Angew. Chem.* **2003**, *115*, 1413; *Angew. Chem. Int. Ed.* **2003**, *42*, 1375; g) Z. Cheng, D. L. J. Thorek, A. Tsourkas, *Angew. Chem.* **2010**, *122*, 356; *Angew. Chem. Int. Ed.* **2010**, *49*, 346.

[15] Y. Tamura, F. Watanabe, T. Nakatani, K. Yasui, M. Fuji, T. Komurasaki, H. Tsuzuki, R. Maekawa, T. Yoshioka, K. Kawada, K. Sugita, M. Ohtani, *J. Med. Chem.* **1998**, *41*, 640.

[16] a) M. A. Azagarsamy, P. Sokkalingam, S. Thayumanavan, *J. Am. Chem. Soc.* **2009**, *131*, 14184; b) V. Yesilyurt, R. Ramireddy, M. A. Azagarsamy, S. Thayumanavan, *Chem. Eur. J.* **2012**, *18*, 223.

[17] a) S. Udenfriend, S. Stein, P. Bohlen, W. Dairman, *Science* **1972**, *178*, 871; b) J. L. Seltzer, K. T. Akers, H. Weingarten, G. A. Grant, D. W. McCourt, A. Z. Eisen, *J. Biol. Chem.* **1990**, *265*, 20409.

[18] T. A. Giambernardi, G. M. Grant, G. P. Taylor, R. J. Hay, V. M. Maher, J. J. McCormick, R. J. Klebe, *Matrix Biol.* **1998**, *16*, 483.

[19] In test tube settings, a definite ^{19}F MR image was observed from the sample containing purified MMP2 and **3a** in the absence of inhibitor **6** (Figure S6 in the Supporting Information).

[20] The ^{19}F MR images shown in Figure 4c were obtained by accumulating 57600 scans for excellent contrast.

[21] M. Tafani, L. Schito, L. Pellegrini, L. Villanova, G. Marfe, T. Anwar, R. Rosa, M. Indelicato, M. Fini, B. Pucci, M. A. Russo, *Carcinogenesis* **2011**, *32*, 1167.

[22] A. E. Kossakowska, D. R. Edwards, C. Prusinkiewicz, M. C. Zhang, D. Guo, S. J. Urbanski, T. Grogan, L. A. Marquez, A. Janowska-Wieczorek, *Blood* **1999**, *94*, 2080.

[23] J. Liao, J. C. Wolfman, A. Wolfman, *J. Biol. Chem.* **2003**, *278*, 31871.

[24] H. J. Zhang, W. Zhao, S. Venkataraman, M. E. C. Robbins, G. R. Buettner, K. C. Kregel, L. W. Oberley, *J. Biol. Chem.* **2002**, *277*, 20919.

Received: March 2, 2013
Revised: June 15, 2013
Published online: ■■ ■■, 0000

Enzyme imaging

*K. Matsuo, R. Kamada, K. Mizusawa, H. Imai, Y. Takayama, M. Narazaki, T. Matsuda, Y. Takaoka, I. Hamachi** ..... ▮▮▮▮–▮▮▮▮

Specific Detection and Imaging of Enzyme Activity by Signal-Amplifiable Self-Assembling ^{19}F MRI Probes

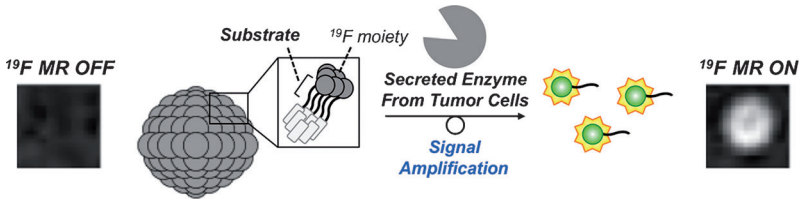

MR imaging probes: New signal-amplifiable self-assembling ^{19}F NMR/MRI probes for turn-on detection and imaging of specific enzymatic activity are reported. The probes are "silent" when aggregated, but exhibit a disassembly-driven turn-on signal change upon cleavage of their substrate part by nanomolar concentrations of the enzyme. Our turn-on probes can be used to visualize the activity of endogenously secreted matrix metalloproteinases from tumor cells (see graphic).

